Journal of Solid State Chemistry **167,** 393–401 (2002)
doi:10.1006/jssc.2002.9677

Synthesis, Crystal Structure, Magnetism, and Optical Properties of $Gd_3[SiON_3]O$—An Oxonitridosilicate Oxide with Noncondensed $SiON_3$ Tetrahedra

Henning A. Höppe,* Gunter Kotzyba,* Rainer Pöttgen,† and Wolfgang Schnick*,[1]

*Department Chemie, Ludwig-Maximilians-Universität München, Butenandtstraße 5–13 (Haus D), D–81377 München, Germany; and †Institut für Anorganische und Analytische Chemie, Westfälische Wilhelms-Universität Münster, Wilhelm-Klemm-Straße 8, D–48149 Münster, Germany

Received February 28, 2002; in revised form May 21, 2002; accepted May 28, 2002

DEDICATED TO GALEN D. STUCKY ON THE OCCASION OF HIS 65TH BIRTHDAY

The novel oxonitridosilicate oxide (sion oxide) $Gd_3[SiON_3]O$ was obtained by the reaction of gadolinium metal with its carbonate oxide and silicon diimide in a radiofrequency (r.f.) furnace at a temperature of 1400°C. The crystal structure of $Gd_3[SiON_3]O$ (*I*4/*mcm*, $a = 649.1(2)$ pm, $c = 1078.8(6)$ pm, $Z = 4$, $R_1 = 0.0411$, $wR_2 = 0.0769$, 405 F^2 values, 19 parameters, 123 K) is isotypic with that of $Ba_3[SiO_4]O$ and $Cs_3[CoCl_4]Cl$. It can be derived from the perovskite structure type by a hierarchical substitution: $Ti^{4+} \rightarrow O^{2-}$, $O^{2-} \rightarrow Gd^{3+}$, $Ca^{2+} \rightarrow [SiON_3]^{7-}$ resulting in the formation of large $[OGd_6]^{16+}$ octahedra, which are twisted by $\xi = 16.47(1)°$ around [001]. The low-temperature single-crystal data investigation led to a crystallographic splitting of the central O atom which could not be resolved at room temperature. The UV–Vis absorption spectra in reflection geometry of the yellow title compound revealed two overlaying broad bands, one peaking at almost the same wavelength as observed in gadolinium oxide (340 nm) and a second red-shifted band at approximately 400 nm indicating a strong influence of nitrogen on the ligand field splitting of the 5*d* states of Gd^{3+}. Temperature-dependent magnetic susceptibility measurements of $Gd_3[SiON_3]O$ show Curie–Weiss behavior from 2 to 300 K with an experimental magnetic moment of 7.68(5) μ_B/Gd, indicating trivalent gadolinium. There is no evidence for magnetic ordering down to 2 K. According to the paramagnetic Curie temperature of −7(1) K, the exchange between the gadolinium magnetic moments is supposed to be only weak. The vibrational spectroscopic data (IR and Raman) are reported. © 2002 Elsevier Science (USA)

Key Words: **gadolinium; oxonitridosilicate; crystal structure; magnetism; UV–Vis spectroscopy; vibrational spectroscopy.**

INTRODUCTION

Nitridosilicates are derived from the classical oxosilicates (which are made up of SiO_4 tetrahedra) by a formal exchange of oxygen by nitrogen. Thus, they contain SiN_4 tetrahedra. This substitution results in a significant extension of the structural possibilities (1, 2). Oxonitridosilicates (so-called "sions") represent an intermediate class of compounds between oxosilicates and nitridosilicates. During the last few years, we developed a synthetic route towards sions and sialons using $SrCO_3$ as an appropriate oxygen source (3). In this paper, we report on the synthesis of a new sion using gadolinium carbonate instead of $SrCO_3$.

The crystal structure of the recently synthesized oxonitridosilicate oxide $Ce_4[Si_4O_4N_6]O$ consists of complex $[Ce_4O]^{10+}$ cations encased by a hyperbolical layer $[Si_4O_4N_6]^{10-}$ (4). Compounds containing oxygen centered tetrahedral $[OM_4]^{n+}$ cations have been found frequently (5). Structures containing oxygen-centered octahedra are also well known. For example $[OM_6]^{4+}$ (M = K, Cs, Rb) in M_3AuO (6), $[OCa_6]^{10+}$ in $Ca_5[WN_4]O_2$ (7), $[OBa_6]^{10+}$ in $Ba_3[SiO_4]O$ (8, 9), $Ba_{11}KX_7O_2$ (X = P, As) (10), $Ba_3In_2Zn_5O_{11}$ (11), $Ba_6Lu_4Zn_{10}O_{22}$ (12), and in inverse perovskite-type Ba_3XO (X = Ge, Si) (13). $[OV_6]$ octahedra which are stabilized by μ^4-Te^{2-} and μ^3-Se^{2-} are found in $KV_3Te_3O_{0.42}$ (14) and $V_6Se_8O(PMe_3)_6$ (15), respectively.

The herein described new sion $Gd_3[SiON_3]O$ contains distorted oxygen-centered octahedra $[OGd_6]$ which carry a high formal charge 16+ if viewed as an isolated complex cation.

EXPERIMENTAL PROCEDURE

Synthesis of Silicon Diimide "$Si(NH)_2$"

Using "$Si(NH)_2$" instead of the relatively unreactive Si_3N_4 as starting material proved to be advantageous for

[1]To whom correspondence should be addressed. Fax: +49-89-2180-7440. E-mail: wolfgang.schnick@uni-muenchen.de.

0022-4596/02 $35.00

the synthesis of the nitridosilicates and this also holds for the sions and sialons (1–3). "$Si(NH)_2$" was obtained by ammonolysis of $SiCl_4$ in CH_2Cl_2 followed by a thermal treatment at 600°C under an atmosphere of pure NH_3:

$$SiCl_4 + 6NH_3 \xrightarrow[NH_3\ \text{atmosphere}]{-78^\circ C} \text{"}Si(NH)_2\text{"} + 4NH_4Cl$$
$$\xrightarrow[NH_3\ \text{atmosphere}]{600^\circ C, -NH_4Cl} \text{"}Si(NH)_2\text{"}. \quad [1]$$

A detailed description of the synthesis of "$Si(NH)_2$" is given in Ref. (3). "$Si(NH)_2$" was yielded as an X-ray amorphous and relatively undefined but reactive product which is converted to amorphous Si_3N_4 at temperatures above 900°C. It is an important precursor for the technical production of Si_3N_4 ceramics (16).

Synthesis of $Gd_3[SiON_3]O$

Under nitrogen atmosphere, $Gd_2(CO_3)_3 \cdot nH_2O$ (STREM chemicals, 99.99%) was dehydrated and partially decarbonated (17) at 500°C according to Eq. (2). A DTA analysis revealed a weight loss of 20.2% corresponding to $n = 5$ and approximately $\frac{1}{2}CO_2$ in agreement with Ref. (17):

$$Gd_2(CO_3)_3 \cdot 5H_2O \rightarrow Gd_2(CO_3)_{2,5}O_{0,5} + \tfrac{1}{2}CO_2 + 5H_2O. \quad [2]$$

In an argon-filled glove box 244 mg (0.496 mmol) of this dehydrated product, 240.9 mg (1.532 mmol) Gd metal (average particle size $\approx$0.5 mm, chempur, 99.9%) and 58.1 mg silicon diimide were thoroughly mixed. The synthesis of $Gd_3[SiON_3]O$ was performed in a radio-frequency (r.f.) furnace under a nitrogen atmosphere according to Eq. (3). The mixture was heated to 1000°C within 5 min and maintained at this temperature for 25 min before further heating to 1400°C within 12 h and maintained at this temperature for 8 h. Then the mixture was cooled down to 600°C within 5 h. Further details about the experimental setup are given in Refs. (3, 18). $Gd_3[SiON_3]O$ was obtained as a coarsely crystalline yellowish main product besides colorless Gd_2O_3. The title compound could easily be separated from the by-product due to their differing crystal habit and color. Due to the low degree of condensation the product undergoes slow hydrolysis in humid air:

$$14Gd_2(CO_3)_{2,5}O_{0,5} + 12\text{"}Si(NH)_2\text{"} + 20Gd + 6N_2$$
$$\rightarrow 12Gd_3[SiON_3]O + 6Gd_2O_3 + 12H_2 + 35CO_2. \quad [3]$$

The results of the EDX analysis revealed a molar ratio of Gd:Si = 3:1. The elemental analysis (Pascher, Remagen, precision $\approx$0.5% (O, N), $\approx$0.5% (Si), $\approx$1.0% (Gd)) fairly agrees with the theoretical values (in brackets): Gd 80.3 wt% (82.2%), Si 4.8% (4.9%), O 5.8% (5.6%), N 9.1% (7.3%). There was no evidence of a phase width of the compound.

UV–Vis Measurements

For the measurement of UV–Vis absorption spectra in reflection geometry, a Hitachi U-3501 spectrophotometer was used. The spectra were recorded at room temperature between 300 and 700 nm. Below 300 nm, the background absorption of the object slide on which the samples were fixed grew rapidly.

Magnetic Measurements

Temperature-dependent magnetic susceptibility data of a polycrystalline, powdered sample of $Gd_3[SiON_3]O$ were measured with an MPMS *XL* SQUID magnetometer (Quantum Design) from 2 to 300 K with magnetic flux densities up to 5 T. A quantity of 6.645 mg (identical sample as used for powder X-ray diffraction) was enclosed in a silica tube and fixed at the sample holder rod. The sample was then cooled to 2 K in zero magnetic field and slowly heated to room temperature in an applied external field.

Vibrational Spectroscopy

FTIR spectra were obtained at room temperature by using a Bruker IFS 66v/S spectrometer. The samples were thoroughly mixed with dried KBr (5 mg sample, 500 mg KBr). Raman spectra were excited by a Bruker FRA 106/S module with an Nd–YAG laser ($\lambda = 1064$ nm) scanning a range from 100 to 3500 cm^{-1}. All sample preparations have been performed in a glove box under dried argon atmosphere.

CRYSTAL STRUCTURE ANALYSIS AND LATTICE ENERGY CALCULATIONS

Crystal Structure Analysis at $T = 293$ K

X-ray diffraction data of the title compound $Gd_3[SiON_3]O$ were collected on a Stoe Stadi4 four-circle diffractometer using Mo$K\alpha$ radiation: The single crystal was enclosed in a silica tube (0.2 mm) sealed under argon atmosphere. The diffraction data were corrected for an intensity decay (+9%). According to the observed extinction conditions (all reflections hkl with $h + k + l = 2n$, $hk0$ with $h + k = 2n$, $0kl$ with $k, l = 2n$, hhl with $l = 2n$, and $00l$ with $l = 2n$) the space groups $I4/mcm$, $I4cm$, and $I\bar{4}c2$ were taken into account. The structure solution and refinement was only possible using space group $I4/mcm$ (no. 140).

The crystal structure of $Gd_3[SiON_3]O$ was solved by direct methods using SHELXTL (19) and refined with anisotropic displacement parameters for all atoms. The relevant crystallographic data and further details of the X-ray data collection are summarized in Table 1. Table 2

TABLE 1
Crystallographic Data of $Gd_3[SiON_3]O$ (e.s.d's. in Parentheses) for the Refinement at 293 K

Crystal Data	
$Gd_3[SiON_3]O$	$F(000) = 972$
$M = 573.87$ g/mol	$\rho = 8.355$ g/cm
Tetragonal	Mo$K\alpha$-radiation
Space group $I4/mcm$ (no. 140)	$\lambda = 71.073$ pm
$a = 650.4(2)$ pm	$\mu = 43.25\ mm^{-1}$
$c = 1079.2(7)$ pm	$T = 293(2)$ K
$V = 456.5(4) \times 10^6\ pm^3$	Block
	$0.083 \times 0.074 \times 0.069\ mm^3$
$Z = 4$	Yellow
Data collection (293 K)	
Stoe STADI4	Measured octants: all
Absorption correction: numerical (ψ-scans)	$h = -6 \rightarrow 6$
	$k = -6 \rightarrow 6$
$T_{min} = 0.0849$; $T_{max} = 0.1287$	$l = -11 \rightarrow 11$
$R_{int} = 0.0672$	93 independent reflections
$2\theta_{max} = 44.9°$	84 observed reflections ($F_o^2 \geq 2\sigma(F_o^2)$)
Refinement (293 K)	
Refinement on F^2	Program used to refine structure: SHELXL-97 (19)
$R_1 = 0.0215$ (all data)	$w^{-1} = \sigma^2 F_o^2 + (xP)^2 + yP$; $P = (F_o^2 + 2F_c^2)/3$
$wR_2 = 0.0324$ (all data)	Weighting scheme (x/y) 0.0141/0
GooF = 1.211	Extinction coefficient: 0.0019(2)
2063 measured reflections	Min. residual electron density: $-0.702\ eÅ^{-3}$
18 parameters	Max. residual electron density: $0.991\ eÅ^{-3}$
Powder diffraction (Rietveld refinement of the lattice parameters)	
$Gd_3[SiON_3]O$	Program used to refine lattice parameters: GSAS (20)
Mo$K\alpha$-radiation	
$a = 650.66(2)$ pm	$wR_p = 0.0745$
$c = 1079.99(3)$ pm	$R_p = 0.0578$
$V = 457.23(2) \times 10^6\ pm^3$	$R_{F^2} = 0.0762$
	$R_F = 0.0548$
	$\chi^2 = 0.8468$
	198 reflections ($2\theta_{max} = 60.0°$)

shows the positional and displacement parameters for all atoms. In Table 5, selected interatomic distances and angles are listed. Furthermore, all reflections detected by X-ray powder diffraction (Stoe Stadi P) of single-phase $Gd_3[SiON_3]O$ have been indexed and their observed intensities are in good agreement with the calculated diffraction pattern based on the single-crystal data. The Rietveld refinement of the lattice parameters (Table 1) has been performed with the program GSAS (20). The powder diffraction pattern of $Gd_3[SiON_3]O$ is shown in Fig. 1. The asterisk in Fig. 1 indicates the strongest reflection of the by-product Gd_2O_3. A two-phase refinement yielded a content of this by-product of ca. 1%.

Due to their identical electronic configuration and their very similar atomic form factors, the unequivocal differentiation of N^{3-}/O^{2-} by X-ray diffraction is not reliable. Therefore, the assignment of the Gd, Si, O and N atoms to their crystallographic positions in $Gd_3[SiON_3]O$ was checked by lattice energy calculations using the MAPLE concept (MAPLE = Madelung Part of Lattice Energy) (21–23). To our experience, MAPLE calculations usually are an appropriate tool to analyze O/N distributions in oxonitrides, and in several cases we have been able to confirm these results by neutron diffraction (4, 24). The results of these calculations are summarized in Table 6. They are in very good agreement with the expected data.

Further details of the crystal structure investigations reported in this paper may be obtained from the Fachinformationszentrum Karlsruhe, D–76344 Eggenstein-Leopoldshafen, Germany, by quoting the depository number CSD–412373 (investigation at 293 K) and CSD–412374 (investigation at 123 K).

The crystal structure of $Gd_3[SiON_3]O$ is isotypic with that of $Ba_3[SiO_4]O$ (8, 9) and $Cs_3[CoCl_4]Cl$ (25) and it derives from perovskite $CaTiO_3$ by hierarchical substitution: $Ti^{4+} \rightarrow O^{2-}$, $O^{2-} \rightarrow Gd^{3+}$, $Ca^{2+} \rightarrow [SiON_3]^{7-}$. The resulting OGd_6 octahedra are subsequently twisted by $\xi = 16.47(1)°$ around [001]. In conclusion, the crystal structure of $Gd_3[SiON_3]O$ consists of corner-sharing OGd_6 octahedra which are elongated along [001]. The resulting large vacancies are filled by non-condensed $SiON_3$ tetrahedra (Figs. 2 and 3).

The twisting of the above-mentioned elongated $[OGd_6]^{16+}$ octahedra presumably is caused by electrostatic reasons or size effects. In perovskite, Ca^{2+} is surrounded by 12 O^{2-} ions. Contrarily in $Gd_3[SiON_3]O$ the formal Si^{4+}, although shielded in their $SiON_3$ tetrahedra, are surrounded by 12 Gd^{3+} ions as second next neighbors leading to an electrostatic repulsion. Because of the twisting, four out of 12 Si–Gd distances become extensively larger resulting in 401.9(1) pm ($4 \times$ Si–Gd2) compared with 314.7(2) pm ($4 \times$ Si–Gd2) and 325.2(1) pm ($4 \times$ Si–Gd1), respectively. A similar effect has been observed in Ba_3MO (M = Ge, Si) (13). Additionally, the O–Gd2 distances (239.8(1) pm) are slightly shortened (O–Gd1: 269.8(2) pm) and thus the elongation of the OGd_6 octahedra is achieved and the distances fit better into the range of typical O–Gd distances (226.2–238.5 pm in Gd_2O_3 (26), sum of the ionic radii ($Gd^{[8]}$): 240–246 pm (27)). The Gd^{3+} are coordinated ten- and eight-fold, respectively; the coordination spheres are shown in Fig. 4. The distances $Gd1^{[10]}$–X (X = O, N) range between 269.8(2) and 273.9(7) pm, while in contrast the distances $Gd2^{[8]}$–X (X = O, N) are distributed quite heterogeneously between 231(1) and 261.9(9) pm.

TABLE 2
Atomic Coordinates and Anisotropic Displacement Parameters for $Gd_3[SiON_3]O$ (e.s.d's. in Parentheses) for the Refinement at 293 K

Atom	Wyckoff symbol	f. o. f.[a]	x	y	z	U_{11}	U_{22}	U_{33}	U_{23}	U_{13}	U_{12}	U_{eq}
Gd(1)	4*a*		0	0	$\frac{1}{4}$	217(7)	217(7)	130(9)	0	0	0	188(6)
Gd(2)	8*h*		0.67611(9)	0.17611(9)	0	83(5)	83(5)	75(6)	0	0	−4(4)	81(5)
Si(1)	4*b*		0	$\frac{1}{2}$	$\frac{1}{4}$	90(26)	90(26)	77(41)	0	0	0	85(16)
N(1)	16*l*	0.75	0.141(2)	0.641(2)	0.1478(9)	352(40)	352(40)	146(51)	31(43)	31(43)	−132(72)	283(27)
O(1)	16*l*	0.25	0.141(2)	0.641(2)	0.1478(9)	352(40)	352(40)	146(51)	31(43)	31(43)	−132(72)	283(27)
O(2)	4*c*		0	0	0	173(77)	173(77)	1241(257)	0	0	0	529(81)

[a] f. o. f. = fractional occupancy factor.
Note. The anisotropic temperature factor is given as $\exp[-2\pi^2(U_{11}h^2a^{*2} + \cdots + 2U_{13}hla^*c^*)]$. U_{eq} is defined as one-third of the trace of the U_{ij} tensor.

The exact symmetry reduction starting from perovskite down to $Gd_3[SiON_3]O$ starts from space group $Pm\bar{3}m$ (no. 221) via a $k2$ transition to $Fm\bar{3}c$ (no. 226); an example for a similar phase crystallizing in the latter space group is $Sr_2Fe_2O_5$ (only $\frac{5}{6}$ of the O-position are occupied) (28). Subsequent $t3$ transition leads to the space group of the herein described gadolinium sion oxide, viz. $I4/mcm$. Further details relating to this discussion are presented in Table 7. In all the three discussed isotypic phases, the octahedra are elongated with a deviation from the average X–M distance (in the respective XM_6 octahedron) of 2.2% in $Ba_3[SiO_4]O$ (OBa_6), 2.4% in $Cs_3[CoCl_4]Cl$ ($ClCs_6$), and 5.3% in $Gd_3[SiON_3]O$ (OGd_6), respectively. As this elongation is the largest for $Gd_3[SiON_3]O$, it seemed possible that a crystallographic splitting of the central oxygen atom in the OGd_6 octahedron occurs at lower temperatures. Therefore, an investigation at $T = 123$ K was carried out.

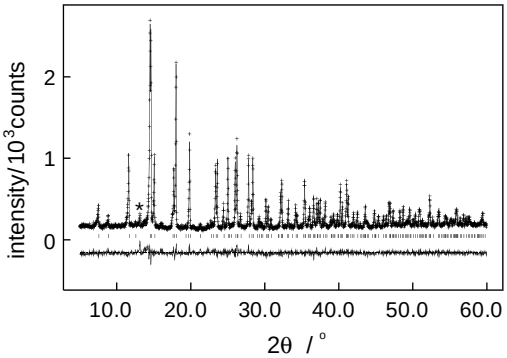

FIG. 1. Observed (crosses) and calculated (line) X-ray powder diffraction pattern (Mo$K\alpha$ radiation) as well as the difference profile of the Rietveld refinement of $Gd_3[SiON_3]O$. The row of vertical lines indicates possible peak positions of $Gd_3[SiON_3]O$. The asterisk at $2\theta = 13.0°$ represents the strongest reflection of the by-product Gd_2O_3.

Crystal Structure Analysis at T = 123 K

X-ray diffraction data of the title compound $Gd_3[SiON_3]O$ were collected on a Stoe Stadi4 four-circle diffractometer using Mo$K\alpha$ radiation. Both at $T = 123$ and $T = 293$ K the same extinction conditions were observed.

The structure solution and refinement was again only possible in space group $I4/mcm$ (no. 140). The crystal structure of $Gd_3[SiON_3]O$ was solved by direct methods using SHELXTL (19) and refined with anisotropic displacement parameters for all atoms. The relevant crystallographic data and further details of the X-ray data collection are summarized in Table 3. Table 4 shows the positional and displacement parameters for all atoms. In Table 5, selected interatomic distances and angles are listed.

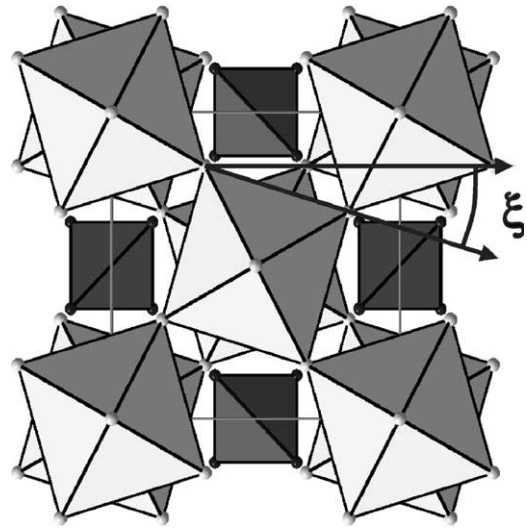

FIG. 2. Crystal structure of $Gd_3[SiON_3]O$ viewed along [001]; the $SiON_3$ tetrahedra are shown as closed dark polyhedra and the OGd_6 octahedra are shown as closed bright polyhedra; the twisting angle ξ is indicated.

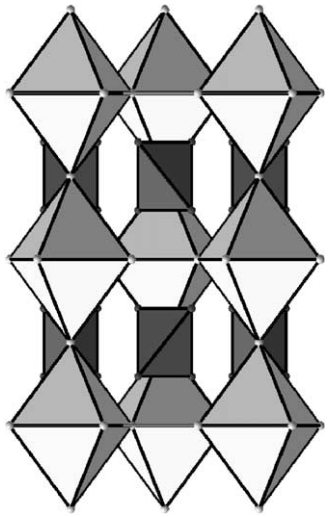

FIG. 3. Crystal structure of $Gd_3[SiON_3]O$ viewed along [010]; the $SiON_3$ tetrahedra are shown as closed dark polyhedra and the OGd_6 octahedra are shown as closed bright polyhedra.

TABLE 3
Crystallographic Data of $Gd_3[SiON_3]O$ (e.s.d's. in Parentheses) for the Refinement at 123 K

Crystal data	
$Gd_3[SiON_3]O$	$F(000) = 972$
$M = 573.87$ g/mol	$\rho = 8.387$ g/cm
Tetragonal	Mo$K\alpha$-radiation
Space group $I4/mcm$ (no. 140)	$\lambda = 71.073$ pm
$a = 649.1(2)$ pm	$\mu = 43.25\ mm^{-1}$
$c = 1078.8(6)$ pm	$T = 123(2)$ K
$V = 454.5(3) \times 10^6\ pm^3$	Block
	$0.211 \times 0.149 \times 0.080\ mm^3$
$Z = 4$	Yellow
Data collection (123 K)	
Stoe STADI4	Measured octants: all
Absorption correction:	$h = -11 \rightarrow 11$
numerical (ψ-scans)	$k = -11 \rightarrow 11$
$T_{min} = 0.0317$; $T_{max} = 0.0769$	$l = -19 \rightarrow 19$
$R_{int} = 0.1275$	405 independent reflections
$2\theta_{max} = 79.9°$	360 observed reflections ($F_o^2 \geq 4\sigma(F_o^2)$)
Refinement (123 K)	
Refinement on F^2	Program used to refine structure: SHELXL-97 (19)
$R_1 = 0.0411$ (all data)	$w^{-1} = \sigma^2 F_o^2 + (xP)^2 + yP$; $P = (F_o^2 + 2F_c^2)/3$
$wR_2 = 0.0769$ (all data)	Weighting scheme (x/y) 0.0202/20.1403
GooF = 1.250	Extinction coefficient: 0.0157(9)
13 019 measured reflections	Min. residual electron density: $-2.78\ eÅ^{-3}$
19 parameters	Max. residual electron density: $2.62\ eÅ^{-3}$

The structure was also refined using space group $I4\,cm$ (no. 108) which requires the same extinction conditions as the chosen space group $I4/mcm$ (no. 140) to avoid the crystallographic splitting of atom O(2), but this did not lead to better R values and satisfactory results. Also the refined Flack parameter could not be determined reliably and it was impossible to determine reasonable anisotropic displacement parameters for all atoms.

Because of the statistical assignment of O/3N to the anionic position of the SiX_4 tetrahedron, it seemed possible that there might be a superstructure with an ordered distribution of $SiON_3$ tetrahedra. Furthermore, the absence of body centering of several M_3BX_5 phases has been intensively discussed in the past (see Refs. (8, 9, 25); hence, we focussed carefully on these points. The unit cell and the extinction conditions were confirmed by a complete set of precession photographs. Reflections indicating a superstructure have not been detected.

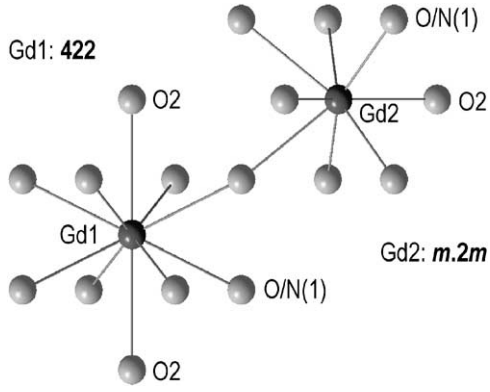

FIG. 4. Coordination of the Gd atoms in $Gd_3[SiON_3]O$ at 293 K; the respective site symmetries are indicated.

At $T = 123$ K, a crystallographic splitting of O(2) was found. The resulting distances O(2)–Gd are almost equal and the coordination environment of O(2) can be described as a square pyramid. The angle Gd(1)–O(2)–Gd(2) is slightly increased from 90° (293 K) to 96.7(5)°. At room temperature, this crystallographic splitting could not be resolved and accordingly elongated OGd_6 octahedra are observed (Fig. 5).

OPTICAL PROPERTIES

UV–Vis Spectroscopy

The energy level scheme of Gd^{3+} is well known (29) and as Gd^{3+} being isoelectronic with Eu^{2+} similar UV–Vis spectra showing very broad bands are observed. But in contrast to Eu^{2+} where the transition between its ground state $4f^7$ and the excited state $4f^6\ 5d^1$ is normally observed in the visible region, Gd^{3+}-containing

TABLE 4
Atomic Coordinates and Anisotropic Displacement Parameters for $Gd_3[SiON_3]O$ (e.s.d's. in Parentheses) for the Refinement at 123 K

Atom	Wyckoff symbol	f. o. f.[a]	x	y	z	U_{11}	U_{22}	U_{33}	U_{23}	U_{13}	U_{12}	U_{eq}
Gd(1)	4*a*		0	0	$\frac{1}{4}$	187(3)	187(3)	120(4)	0	0	0	165(3)
Gd(2)	8*h*		0.67590(6)	0.17590(6)	0	75(2)	75(2)	74(3)	0	0	−1(2)	75(2)
Si(1)	4*b*		0	$\frac{1}{2}$	$\frac{1}{4}$	90(11)	90(11)	68(15)	0	0	0	83(7)
N(1)	16*l*	0.75	0.142(2)	0.642(2)	0.1479(8)	318(31)	318(31)	113(26)	25(20)	25(20)	−193(41)	250(20)
O(1)	16*l*	0.25	0.142(2)	0.642(2)	0.1479(8)	318(31)	318(31)	113(26)	25(20)	25(20)	−193(41)	250(20)
O(2)	8*f*	0.5	0	0	0.026(2)	156(44)	156(44)	185(93)	0	0	0	166(34)

[a] f. o. f. = fractional occupancy factor.
Note. The anisotropic temperature factor is given as $\exp[-2\pi^2(U_{11}h^2a^{*2} + \cdots + 2U_{13}hla^*c^*)]$. U_{eq} is defined as one-third of the trace of the U_{ij} tensor.

compounds are usually colorless. In Contrast to the 4*f*-states, the 5*d*-states are strongly influenced by the coordination sphere in the host lattice; due to the nephelauxetic effect (N^{3-}/O^{2-}) the ligand field splitting of the 5*d*-levels is expected to become larger and in consequence the observed transitions are red shifted. This has been convincingly shown for Ce^{3+}-doped Y–Si–O–N compounds (30) or Eu^{2+}-doped $Ba_2[Si_5N_8]$ (31). And this also holds for $Gd_3[SiON_3]O$ which has a yellowish color. Thus, the optical reflectance spectra were measured (Fig. 6). These revealed two overlaying broad bands, one peaking at almost the same wavelength as observed in gadolinium oxide (340 nm) and a second red-shifted band at approximately 400 nm.

TABLE 5
Selected Interatomic Distances (pm) and Angles (deg) for $Gd_3[SiON_3]O$ at 293 and 123 K, Respectively (e.s.d's. in Parentheses)

		Measurement at 293 K	Measurement at 123 K
Gd(1)	–O(2)[0] (2 ×)	269.8(2)	241(2), 298(2)
	–O(1)[1]/N(1)[1] (8 ×)	273.9(7)	273.0(6)
Gd(2)	–O(1)[1]/N(1)[1] (2 ×)	231(1)	230.6(9)
	–O(2)[0] (2 ×)	239.8(1)	241.0(3)
	–O(1)[1]/N(1)[1] (4 ×)	261.9(9)	262.0(8)
	–Gd(2)		322.9(1)
	–Gd(1)		360.6(1)
Si(1)	–O(1)[1]/N(1)[1] (4 ×)	171(1)	171.1(9)
O(1)/N(1)	–Si(1)[4]	171(1)	171.1(9)
	–Gd(2)[8]	231(1)	230.6(9)
	–Gd(2)[8] (2 ×)	261.9(9)	262.0(8)
	–Gd(1)[10] (2 ×)	273.9(7)	273.0(6)
O(2)	–O(2)[0]	—	56(4)
	–Gd(2)[8] (4 ×)	239.8(1)	241.0(3)
	–Gd(1)[10]	269.8(2)	241(2)
	–Gd(1)[10]	269.8(2)	298(2)
$O^{[1]}/N^{[1]}$–Si–$O^{[1]}/N^{[1]}$		99.3(4)–114.7(4)	99.8(6)–114.5(4)

Vibrational Spectroscopy

Normally, the vibrations of SiO_4 tetrahedra in orthosilicates range between 1000 and 400 cm^{-1} as observed in olivine (32) or zirconite (33). Valence vibrations are found above 860 cm^{-1}, and deformation modes below 620 cm^{-1}. The Si–N bond is expected to be weaker than the Si–O bond. Thus, the vibrations of the $SiON_3$ tetrahedra in $Gd_3[SiON_3]O$ occur at lower wavenumbers (Fig. 7). Unfortunately, very broad unresolved bands at 885 and

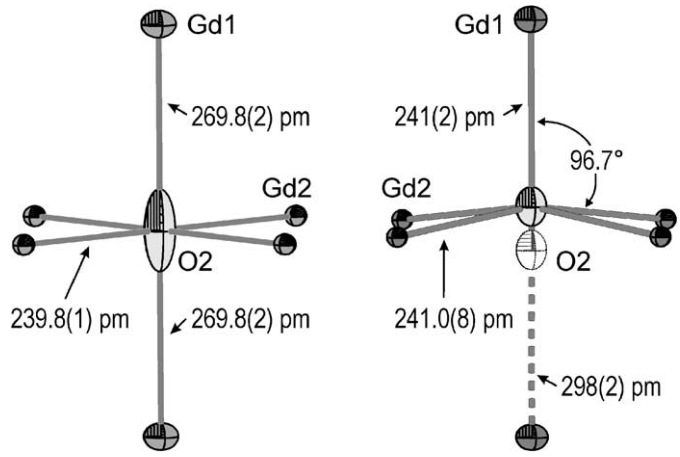

FIG. 5. Coordination of the O2 atom in $Gd_3[SiON_3]O$ at 293 K (left) and 123 K (right, both positions of the crystallographically splitted O2 atom are presented).

TABLE 6
Results of the MAPLE Calculations for $Gd_3[SiON_3]O$ and Increment Calculations in kJ/mol at 293 and 123 K, Respectively

	Measurement at 293 K	Measurement at 123 K
Gd(1)	4350	4462
Gd(2)	4287	4150
Si(1)	9838	9988
O(1)/N(1)	4124	4103
O(2)	1993	1967

Typical partial MAPLE values (in kJ/mol)[a]

MAPLE($3GdN + SiO_2$)	MAPLE($Gd_3[SiON_3]O$) (293 K)		MAPLE($Gd_3[SiON_3]O$) (123 K)	
41 598	41 721	$\Delta^b = 0.3\%$	41440	$\Delta = 0.4\%$

[a] Gd^{3+}: 3900–4550; Si^{4+}: 9000–10 200; N^{3-}: 5000–6000; O^{2-}: 2000–2800; $(O_{1/4}N_{3/4})^{-2.75}$: 4000–5200.
[b] Δ = difference.

$693\,cm^{-1}$, respectively, are observed and thus a precise assignment is impossible. In the olivine spectra two very strong broad bands have been observed at 1005 and $882\,cm^{-1}$, respectively. Below $600\,cm^{-1}$, the additional vibrations of the OGd_6 units have to be considered and the IR spectrum, becomes very complex. In the Raman spectrum, we observe broad weak bands around 875 and $740\,cm^{-1}$, and two quite sharp bands peaking at 583 and $533\,cm^{-1}$, respectively. In olivine, similar bands have been found at 960, 917, 854 and $822\,cm^{-1}$, respectively.

MAGNETIC PROPERTIES

The temperature dependence of the inverse magnetic susceptibility (0.5 T data) of $Gd_3[SiON_3]O$ is displayed in Fig. 8. Over the whole temperature range we observe Curie–Weiss behavior $\chi = C/(T-\Theta)$ with an experimental magnetic moment of $7.68(5)\,\mu_B/Gd$, close to the free ion value of $7.94\,\mu_B/Gd^{3+}$ (see Ref. (34)). The paramagnetic Curie temperature (Weiss constant) of $\Theta = -7(1)$ K was determined by linear extrapolation of the $1/\chi$ vs T data to $1/\chi = 0$. According to the small Weiss constant, we expect weak antiferromagnetic interactions of the gadolinium magnetic moments at very low temperatures. As presented in Fig. 9, the low-field (0.002 T) zero-field cooling (zfc) and field cooling (fc) measurements gave no indication for magnetic ordering down to 2 K.

CONCLUSIONS

$Gd_3[SiON_3]O$ is one of the rare oxonitridosilicates with a non-condensed Si/O/N substructure. Other examples are $Li_6[SiN_2O_2]$ (35), the silicoapatites $Ln_{10}[SiO_{3.67}N_{0.33}]_6O_2$ (Ln = La, Nd, Sm, Gd) and $M_{10}[SiO_2N_2]_6O_2$ (M = Ti, Ge) (36). The nitrogen atoms are located completely in the SiX_4 tetrahedra. Another example crystallizing isotypic with β-K_2SO_4 are the sions LnEu$[SiO_3N]$ (Ln = La, Nd, Sm) (37). Typically, the materials properties of oxonitridosilicates like inertness against hydrolysis, thermal stability, and mechanical hardness are strongly influenced by the degree of condensation of the Si/O/N substructures. Accordingly, $Gd_3[SiON_3]O$ unlike the higher condensed

TABLE 7
Relevant Data of Perovskite, $Gd_3[SiON_3]O$ and Several Isotypic A_3BX_5 Phases (e.s.d's. in Parentheses)

Compound	a/c ratio	Angle ξ (deg)	Deviation of the resp. XM_6 octahedron
$Gd_3[SiON_3]O$ (293 K)	0.603(1)	16.47(1)	5.3% (X = O, M = Gd)
$Gd_3[SiON_3]O$ (123 K)	0.602(1)	16.51(1)	no octahedron
$Ba_3[SiO_4]O$	0.651	14.96	2.2% (X = O, M = Ba)
$Cs_3[CoCl_4]Cl$	0.635	19.34	2.4% (X = Cl, M = Cs)
$Ca[TiO_3]$ (in a body-centered tetragonal cell setting)	$\sqrt{2}/2 \approx 0.7$	0	None (X = Ti, M = O)

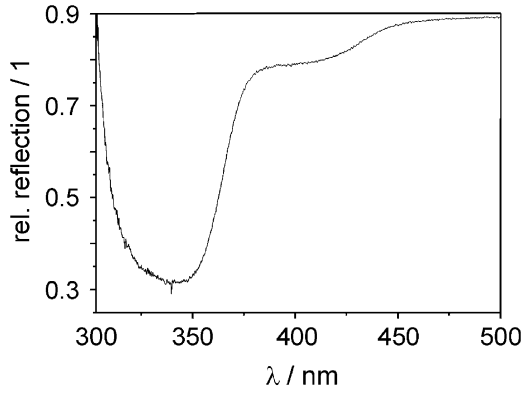

FIG. 6. UV–Vis absorption spectrum of $Gd_3[SiON_3]O$ at 293 K.

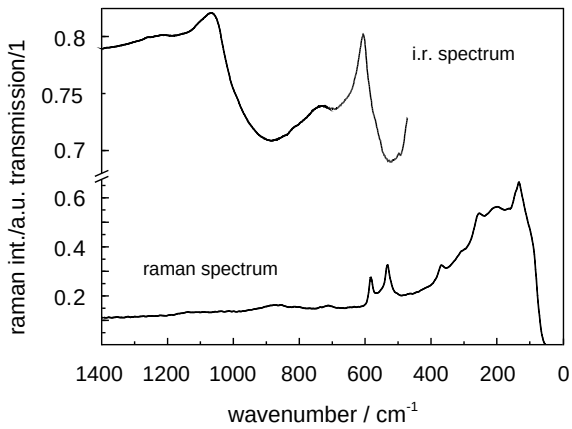

FIG. 7. Infrared vibrational spectrum (top) and Raman spectrum (bottom) of $Gd_3[SiON_3]O$ recorded at room temperature.

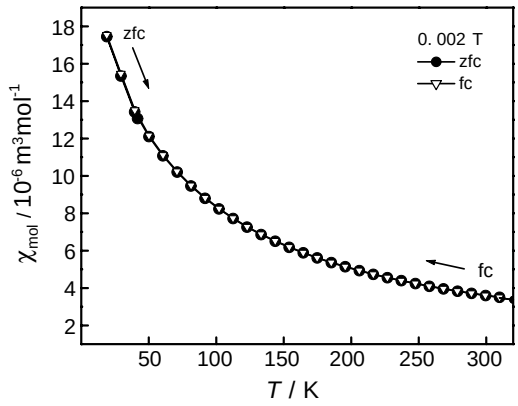

FIG. 9. Low-temperature susceptibility of $Gd_3[SiON_3]O$ measured at an external flux density of 0.002 T in the zfc (black circles) and fc (white triangles) modus.

nitridosilicates and oxonitridosilicates undergoes slow hydrolysis in humid air.

Interestingly, most oxonitridosilicates obtained so far exhibit a rather high degree of condensation of their Si/O/N substructures, and thus they show a high chemical stability against hydrolysis (3). Presumably, the highly condensed network structures are a direct consequence of the severe high-temperature conditions during the synthesis of these compounds in the radiofrequency furnaces. Apparently, only the most stable structures survive these reaction conditions. Due to lattice energetic reasons, the perovskite structure type is fairly stable as well and thus $Gd_3[SiON_3]O$ representing the anti-type is obtained under similar conditions in the radiofrequency furnace. Recently $Ce_{16}[Si_{15}O_6N_{32}]$, another oxonitridosilicate, was described, which represents a superstructure of a defect variant of the perovskite structure type, where most of the octahedra have been substituted by tetrahedra (38).

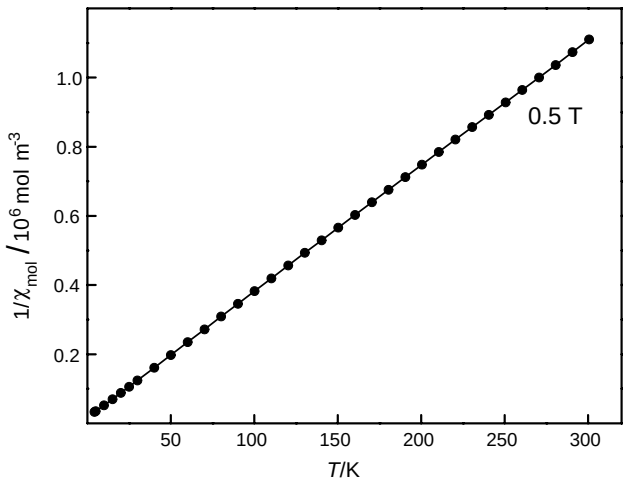

FIG. 8. Temperature dependence of the inverse magnetic susceptibility of $Gd_3[SiON_3]O$ measured at a flux density of 0.5 T.

ACKNOWLEDGMENTS

This work has been supported by the Fonds der Chemischen Industrie and especially by the Deutsche Forschungsgemeinschaft (Schwerpunktprogramm "Nitridobrücken" and Gottfried–Wilhelm–Leibniz-Programm).

REFERENCES

1. W. Schnick and H. Huppertz, *Chem. Eur. J.* **3,** 679 (1997).
2. W. Schnick, T. Schlieper, H. Huppertz, K. Köllisch, M. Orth, R. Bettenhausen, B. Schwarze, and R. Lauterbach, *Phosphorus Sulfur Relat. Elem.* **124/125,** 163 (1997).
3. W. Schnick, H. Huppertz, and R. Lauterbach, *J. Mater. Chem.* **9,** 289 (1999).
4. E. Irran, K. Köllisch, S. Leoni, R. Nesper, P. F. Henry, M. T. Weller, and W. Schnick, *Chem. Eur. J.* **6,** 2714 (2000).
5. S. V. Krivovichev, S. K. Filatov, and T. F. Semenova, *Russ. Chem. Rev.* **67,** 137 (1998).
6. C. Feldmann and M. Jansen, *Z. Anorg. Allg. Chem.* **621,** 201 (1995).
7. P. Höhn and R. Kniep, *Z. Kristallogr.* **215,** 333 (2000).
8. E. Tillmanns and H.-P. Grosse, *Acta Crystallogr. B* **34,** 649 (1978).
9. M. Mansmann, *Z. Anorg. Allg. Chem.* **339,** 52 (1965).
10. M. Lulei, *Z. Anorg. Allg. Chem.* **623,** 1796 (1997).
11. M. Scheikowski and H. Müller-Buschbaum, *Z. Anorg. Allg. Chem.* **619,** 559 (1993).
12. C. Rabbow and H. Müller-Buschbaum, *Z. Anorg. Allg. Chem.* **622,** 100 (1996).
13. B. Huang and J. D. Corbett, *Z. Anorg. Allg. Chem.* **624,** 1787 (1998).
14. E. J. Wu, M. A. Pell, H. S. Hugh, and J. A. Ibers, *J. Alloys Compd.* **278,** 123 (1998).
15. D. Fenske, A. Grissinger, M. Loos, and J. Magull, *Z. Anorg. Allg. Chem.* **598/599,** 121 (1991).
16. H. Lange, G. Wötting, and G. Winter, *Angew. Chem. Int. Ed. Engl.* **30,** 1579 (1991).
17. I. N. Tselik, V. Ya. Shvartsman, and V. D. Fedorenko, *Russ. J. Inorg. Chem.* **13,** 53 (1968).

18. T. Schlieper, W. Milius, and W. Schnick, *Z. Anorg. Allg. Chem.* **621,** 1380 (1995).
19. G. M. Sheldrick, "SHELXTL, V 5.10 Crystallographic System." Bruker AXS Analytical X-ray Instruments Inc., Madison, 1997.
20. R. B. von Dreele and A. C. Larson, "General Structure Analysis System," Los Alamos National Laboratory Report LAUR 86-748, 1990.
21. R. Hoppe, *Angew. Chem. Int. Ed. Engl.* **5,** 95 (1966).
22. R. Hoppe, *Angew. Chem. Int. Ed. Engl.* **9,** 25 (1970).
23. R. Hübenthal, "MAPLE, Program for the Calculation of the Madelung Part of Lattice Energy," University of Gießen, Germany, 1993.
24. R. Lauterbach, E. Irran, P. F. Henry, M. T. Weller, and W. Schnick, *J. Mater. Chem.* **10,** 1357 (2000).
25. H. M. Powell and A. F. Wells, *J. Chem. Soc.* 359 (1935).
26. A. Bartos, K. P. Lieb, M. Uhrmacher, and D. Wiarda, *Acta Crystallogr. B* **49,** 165 (1993).
27. R. D. Shannon and C. T. Prewitt, *Acta Crystallogr. B* **25,** 925 (1969).
28. M. Schmidt and S. J. Campbell, *J. Solid State Chem.* **156,** 292 (2001) (doi:10.1006/ jssc.2000.8998).
29. W. T. Carnall, P. R. Fields, and K. Rajnak, *J. Chem. Phys.* **49,** 4443 (1968).
30. J. W. H. van Krevel, H. T. Hintzen, R. Metselaar, and A. Meijerink, *J. Alloys Compd.* **268,** 272 (1998).
31. H. A. Höppe, H. Lutz, P. Morys, W. Schnick, and A. Seilmeier, *J. Phys. Chem. Solids* **61,** 2001 (2000).
32. V. Hohler and E. Funck, *Z. Naturforsch. B* **28,** 125 (1973).
33. R. Hubin and P. Tarte, *Spectrochim. Acta A* **27,** 683 (1971).
34. H. Lueken, "Magnetochemie," Teubner, Stuttgart, 1999.
35. S. Podsiadlo, *J. Therm. Anal.* **32,** 771 (1987).
36. J. Guyader, F. F. Grekov, R. Marchand, and J. Lang, *Rev. Chim. Miner.* **15,** 431 (1978).
37. R. Marchand, *C. R. Acad. Sci., Ser. IIc: Chim.* **283,** 281 (1976).
38. K. Köllisch and W. Schnick, *Angew. Chem. Int. Ed. Engl.* **38,** 357 (1999).